JOURNAL OF Applied Polymer SCIENCE

Special Issue: Manufacturing of Advanced Biodegradable Polymeric Components

Guest Editors: Prof. Roberto Pantani (University of Salerno) and
Prof. Lih-Sheng Turng (University of Wisconsin–Madison)

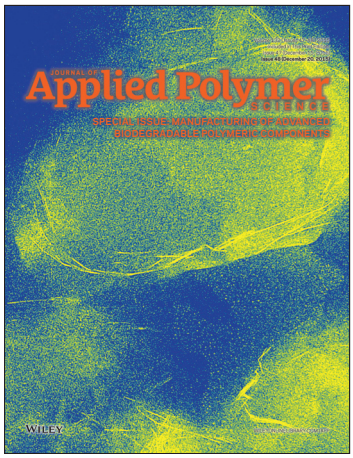

EDITORIAL

REVIEWS

ARTICLES

JOURNAL OF Applied Polymer SCIENCE

Special Issue: Manufacturing of Advanced Biodegradable Polymeric Components

Guest Editors: Prof. Roberto Pantani (University of Salerno) and Prof. Lih-Sheng Turng (University of Wisconsin–Madison)

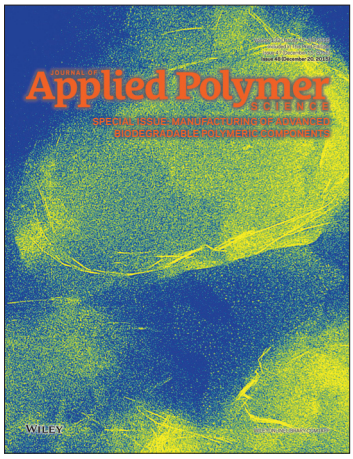

Rotational molding of biodegradable composites obtained with PLA reinforced by the wooden backbone of opuntia ficus indica cladodes
A. Greco and A. Maffezzoli, *J. Appl. Polym. Sci.* 2015, **DOI:** 10.1002/app.42447

Foam injection molding of poly(lactic) acid: Effect of back pressure on morphology and mechanical properties
V. Volpe and R. Pantani, *J. Appl. Polym. Sci.* 2015, **DOI:** 10.1002/app.42612

Modification and extrusion coating of polylactic acid films
H.-Y. Cheng, Y.-J. Yang, S.-C. Li, J.-Y. Hong and G.-W. Jang, *J. Appl. Polym. Sci.* 2015, **DOI:** 10.1002/app.42472

Processing and properties of biodegradable compounds based on aliphatic polyesters
M. R. Nobile, P. Cerruti, M. Malinconico and R. Pantani, *J. Appl. Polym. Sci.* 2015, **DOI:** 10.1002/app.42481

Journal of Applied Polymer Science

Effect of processing techniques on the 3D microstructure of poly (L-lactic acid) scaffolds reinforced with wool keratin from different sources

Debora Puglia,[1] Romina Ceccolini,[1] Elena Fortunati,[1] Ilaria Armentano,[1] Francesco Morena,[2] Sabata Martino,[2] Annalisa Aluigi,[3] Luigi Torre,[1] Jose M Kenny[1]

[1]Civil and Environmental Engineering Department, UdR INSTM, University of Perugia, Terni 05100, Italy
[2]Department of Chemistry, Biology and Biotechnology, University of Perugia, Perugia 06123, Italy
[3]CNR-ISOF, Institute of Organic Synthesis and Photoreactivity, Bologna 40129, Italy
Correspondence to: D. Puglia (E-mail: debora.puglia@unipg.it)

ABSTRACT: The aim of this work was the analysis of morphologies of poly (L-lactic acid)/keratin tridimensional scaffolds developed by using two main solvent based techniques: solvent casting particulate leaching in the presence of paraffin microspheres as porogen, and thermally induced phase-separation process. Keratins from different sources were used. Specifically, keratin from Merino wool (KM) and Brown Alpaca (KA) were dispersed in dioxane or 1,4-dioxane/water mixture and then the keratin structure after interaction with 1.4-dioxane was investigated by means of electrophoresis and spectroscopic analysis. A detailed morphological characterization of the scaffold systems obtained by the two different methods was performed by using field emission scanning electron microscopy. The effect of porogen content, solvent composition and processing parameters, such as the influence of keratin presence (1 wt %) and source (KA and KM) were evaluated. The results reveal that 1,4-dioxane, used as based solvent in the two selected processes, does not negatively affect the keratin structure. A slight change in the procedure parameters, such as porogen content or solvent/non-solvent ratio, significantly affects the resulting porosity and architecture of the obtained PLLA and PLLA/keratin scaffolds. Both keratins can be considered as suitable fillers able to modify the pore architecture and interconnection of three-dimensional PLLA/keratin porous composites obtained by the two different solvent assisted techniques. Of note, both composites are biocompatible, as demonstrated by the culture adult bone-marrow mesenchymal stem cells without signs of toxicity. © 2015 Wiley Periodicals, Inc. J. Appl. Polym. Sci. **2015**, *132*, 42890.

KEYWORDS: biomaterials; biomedical applications; keratin; scaffold; SCPL; TIPS

Received 16 February 2015; accepted 28 August 2015
DOI: 10.1002/app.42890

INTRODUCTION

Keratin is the major component of hair, feathers, nails and horns of mammals.[1] Among these sources, wool keratin emerges as an attractive protein because it is abundant, readily available, and it can be valorized by means of extraction and purification by chemical cleavage of the disulphide bonds of keratin wastes.[2] Protein-based materials have received much attention for application in biomedical fields, in particular in the field of tissue engineering and medical devices.[3,4] Specifically, research on how to extract, purify and characterize keratin from hair, wool fibres, etc., that could lead to the development of keratin-based biomaterials applicable in the field of the tissue engineering, has been carried out. This has resulted in materials that are biodegradable, biocompatible and capable to support cell growth.[5,6]

Tissue engineering is a sector based on the use of degradable materials as tridimensional porous scaffolds. These need to have specific characteristics, e.g., mechanical strength, degradation rate, porosity, controlled microstructure - shape and size – such that they will support cell adhesion and growth, and organ regeneration.[7] Polylactic acid (PLA), polyglycolic acid (PGA), and their copolymers (PLGA) are extensively used, but they do not have specific cell-recognizable signals able to attract seeding and migration of cells.[8,9] In order to improve the ability of these materials to support cell adhesion and proliferation, biomaterials having affinity with the cells, such as keratins, have been used in the preparation of three-dimensional polymeric porous scaffolds.[10–13] In the scaffold design phase, specific characteristics of the scaffolds (other than degradation rate) should also be considered. In order to promote tissue growth, the

scaffolds must have a degradation rate similar to the tissue regeneration rate, and a surface area sufficient to allow cell attachment, ingrowth and penetration. This is done by producing foamed polymeric materials in which the pore size is large enough to permit cell penetration into the pores. In addition, interconnectivity of pores has to be obtained to make possible nutrient and waste exchange by cells.[14] The final characteristics (porosity and pore size) are strictly related to the adopted method selected for scaffold realization. A number of methods have been developed to produce porous 3D architectures, including solvent casting/particulate leaching[15] and phase-separation methods.[16]

In solvent casting/particulate leaching procedures, the polymer is dissolved in an organic solvent by using porogen particles with defined shape and size as inorganic salts, e.g. sodium chloride, sucrose crystals, gelatin or paraffin spheres. The size of the porogen affects the final size of the pores in the scaffold, while the polymer/porogen ratio is directly connected to the amount of porosity of the final tridimensional structure. The main advantage of the solvent casting particulate leaching (SCPL) technique is the easy realization methodology that does not require specialized equipment. The main disadvantages of solvent casting are (1) the limited shapes; (2) the possible presence of retained solvent in the polymer; and (3) denaturation of the proteins included in the solution.[17,18] Resorbable polymeric biomaterials having high porosity values can be also fabricated by using the thermally induced phase separation (TIPS) technique.[19–21] The scaffolds realized with this technique have high porosity with anisotropic tubular morphology and wide pore interconnectivity. Pore morphology and size, mechanical properties, bioactivity and degradation rates of foams realized by the TIPS method can be controlled by varying both polymer and processing parameters.[22,23]

The control over porosity and pore diameter is a function of the solvent choice and phase separating conditions,[20] such as presence of fillers. In detail, filled composite scaffolds can exhibit pore anisotropy that has been shown to support cell migration and adhesion. In addition, bioactive fillers are often used to enhance the targeted biological response and to modify the bulk properties of polymeric scaffolds used in the tissue engineering field.[24]

In this study, porous poly (L-lactic) acid (PLLA) scaffolds were successfully developed by using two main solvent-based techniques: SCPL and TIPS processes. The effect of 1,4-dioxane, keratin structure and processing conditions on final morphologies of poly (L-lactic acid)/keratin tridimensional scaffolds was considered. A detailed morphological analysis was performed, by using FESEM microscopy, and the resulting morphologies were compared on the basis of processing method, solvent dilution and keratin source (keratins extracted from Australian Merino wool (KM) fibres and Brown Alpaca (KA) powders).

Finally, the use of such scaffolds for biological application has been evaluated by culturing adult bone-marrow mesenchymal stem cells on PLLA/keratin derived biocomposites.

EXPERIMENTAL

Materials

PLLA (Molecular weight (M_n) = 120000 g mol^{-1}, polydispersity index (M_w/M_n) = 1.27) was supplied by Purac Biochem. Poly (vinyl alcohol) (PVA) (88% hydrolyzed, average molecular weight 25000 g/mol), paraffin (melting point 53–57°C), 1,4-dioxane, and cyclohexane were purchased from Acros (Belgium). Australian Merino wool (KM) fibres and Brown Alpaca (KA) fibres were selected as keratin sources. Keratins were extracted from Merino wool and Alpaca fibres by using the sulphitolysis reaction previously reported.[2,25] The Mini Protean 3 Cell system, pre-cast polyacrilamide gels and Coomassie Brilliant blue G 250 stain were purchased from Bio-rad, while all other chemicals were purchased from Sigma-Aldrich.

Preparation of PLLA/Keratin Scaffolds

PLLA tridimensional scaffolds were prepared by using the SCPL and TIPS processes (Scheme 1), and the effect of processing procedures on the final morphological behavior of the obtained architectures was deeply investigated and discussed. PLLA/keratin porous scaffolds containing 1 wt % of keratin from Merino wool and Brown Alpaca were also prepared by using two different procedures.

Solvent Casting Particulate Leaching. PLLA tridimensional scaffolds with different porosity and PLLA composite porous scaffolds containing keratins were fabricated with a SCPL process, using paraffin microspheres as porogen.[26] Briefly, paraffin microspheres were prepared by solidifying paraffin drops in PVA solution at 60°C, as previous reported by Li *et al.*[26–28] PLLA was dissolved in 1,4-dioxane by magnetically stirring for 4 h at 65°C and paraffin microspheres were slowly mixed with the PLLA/1,4-dioxane solution at room temperature. The polymer/porogen compositions used for PLLA based scaffolds were 70 wt %, 80 wt % and 90 wt % of porogen with respect of polymer initial weight. The different obtained mixtures were cast on *Teflon*® supports till the complete evaporation of the solvent. After the drying at room temperature, the scaffolds were immersed in 20 mL of cyclohexane in an ultrasonic bath for 45 min to dissolve and remove the paraffin microspheres. The final samples, designed as PLLA_SCPL_70, PLLA_SCPL_80 and PLLA_SCPL_90, accordingly to the porogen content (70, 80, and 90 wt %, respectively), were about 3 mm in thickness.

Composite porous scaffolds loaded with Merino wool (KM) or Brown Alpaca (KA) keratin and with a porogen content of 80 wt % (this value was selected on the basis of morphological properties of neat PLLA scaffolds) were also fabricated with the above mentioned protocol. Firstly, the keratins were sonically dispersed in 1,4-dioxane by an ultrasound tip homogenizer (Vibracell 75043, 750 W, Bioblock Scientific, USA) for 30 min, at 40% of amplitude, in ice bath,[25] then PLLA was added and the procedure continued as reported in the case of neat PLLA. Samples containing 1 wt % of KM or KA keratins with respect of PLLA initial weight, designed as 1KM_SCPL and 1KA_ SCPL, were produced and then morphologically characterized.

Thermally Induced Phase Separation Process. Scaffolds based on neat PLLA and PLLA/keratin composites were prepared by

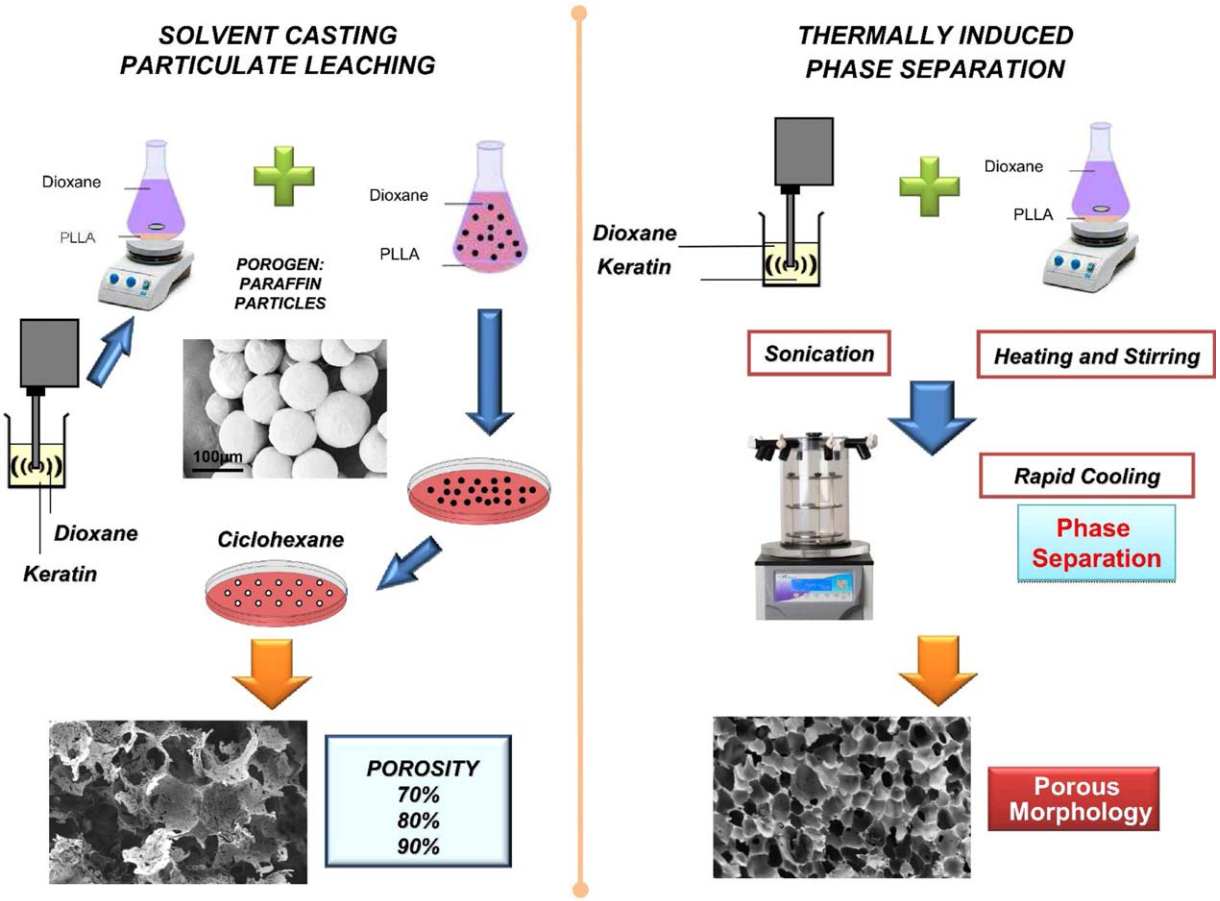

Scheme 1. PLLA/keratin tridimensional scaffolds prepared by SCPL (left) and TIPS processes (right). [Color figure can be viewed in the online issue, which is available at wileyonlinelibrary.com.]

TIPS procedure. Role of the solvent ratio, such as filler type, were investigated. KM or KA were dispersed by using a tip sonicator (Vibracell 75043, 750 W, Bioblock Scientific, USA) in a 90/10 (v/v) or 87/13 (v/v) mixture of 1,4-dioxane/distilled deionized water for 30 min at 40% of amplitude, in ice bath.[25] PLLA was dissolved in the keratin suspension at a temperature above the cloud point (ca. 65°C) by magnetic stirring. The homogeneous dispersion was frozen at −30°C overnight, after that solvents were removed by freeze-drying for 6 days, at a pressure of 10^{-2} mbar and maintained at a temperature of −60°C. Disk-shaped scaffolds of 40 mm in diameter with a thickness of 5 mm were produced. The same process used in the case of keratin loaded systems was considered for the realization of PLLA control scaffolds (namely PLLA_TIPS_90:10 and PLLA_TIPS_87:13), the sample with 100% 1,4-dioxane (PLLA_TIPS_100:0) was also fabricated for comparison. The polymer/solvent ratio was chosen as 10% (w/v). Samples containing 1 wt % of KM or KA respect to PLLA initial weight, respectively designed as 1KM_TIPS and 1KA_TIPS, were prepared by using two different mixtures of 1,4-dioxane and distilled deionized: samples with 90/10 (v/v) were designed as 1KM_TIPS_90:10 and 1KA_TIPS_90:10, while samples with a ratio of 87/13 (v/v) of 1,4-dioxane/water were indicated as 1KM_TIPS_87:13 and 1KA_TIPS_87:13, respectively.

Characterization Methods

Proteins molecular weight distribution was determined by SDS-PAGE according to Laemmli's method.[29] Samples were dissolved at a concentration of 15 mg/mL, in a buffer solution containing Tris/HCl (550 m*M*, pH 8.6), dithiothreitol (DTT, 140 m*M*) and urea (8*M*). The dissolution was carried out under nitrogen atmosphere, overnight.[30] The protein solutions were then diluted to 7.5 mg/mL with the denaturing buffer containing 150 mg of sodium dodecyl sulphate, 0.5 mL of Tris-HCl (0.5*M*, pH 8.6), 1 ml of bromophenol blue (0.5 mg/mL) and glycerine 87% up to 4 mL, and heated at 70°C for 5 minutes. The prepared solutions were run in a 12% polyacrilamide pre-casting gel, using a Mini Protean 3 Cell system from Bio-Rad with at a constant voltage of 200 kV for 1h. Proteins were visualized by Coomassie Brilliant blue R 250 stain.

FT-IR spectra of pristine KM keratin and KM keratin after dissolution in 1,4-dioxane were acquired, in transmission mode, by using a Thermo Nicolet Nexus Spectrometer, by placing the powder dried at 105°C for 1 h, between the NaCl round cell windows. The spectra, recorded in the 4000–650 cm^{-1} range using 20 scans and a resolution of 4 cm^{-1}, were corrected and smoothed with a nine-point Savitsky−Golay function. Resolution of the amide I band was done by means of Gaussian shape

bands related to different protein secondary structures. The results of the fitting procedure were further evaluated by investigating the residual from the difference between fitted and original curve and accepted when the R2 was higher than 0.9900. The morphologies of the raw KM and KA keratins were also investigated by field emission scanning electron microscopy (FESEM, Zeiss, Supra25).

The shape and size of paraffin microspheres, used as porogen in the SCPL process, were analyzed by means of FESEM analysis. Microspheres were deposited on a conductive substrate, gold coated and directly analyzed. The microstructure of the scaffolds produced by the different techniques was also investigated by FESEM and the configuration of the porous architecture in 3D scaffolds was studied by analyzing the pore shape, dimension and their interconnectivity. Both surfaces and cross-sections of PLLA and PLLA/keratin porous formulations were characterized by FESEM and analyzed to study the effect of different process parameters and procedures on internal pore structure, morphology and porosity. Cross-sections were obtained by fracture of the samples after immersion in liquid nitrogen and then gold sputtered. Porosity measurements were performed according to Choudhury *et al.*,[31] while pore size distribution was determined by analyzing FESEM images using Nikon NIS-Elements software.

Biological Characterization of PLLA And PLLA/Keratin Scaffolds

Protein Adsorption. Protein adsorption tests were carried out by transferring 300 μg of bovine serum albumin (BSA, Sigma-Aldrich), 10% fetal bovine serum (FBS, Euroclone) and plasma from normal donor at dilution 1 : 10 on PLLA and PLLA composite surfaces. According to our previous work,[32,33] proteins were incubated for 30 min and 24 h at 37°C. After three washes in distilled H_2O, the total protein content was measured by the Bradford method.[34] Absorbance (595 nm) was measured using a microtiter plate reader (ELISA reader, GDV-DV990BV6, Italy). Every sample was analyzed in five independent experiments, each of which in triplicate. Reported Data are the mean value ± standard error of the mean of each group and are referred to a standard curve using BSA as the reference ($p<0.05$).

Isolation and Culture of Human Bone-marrow Mesenchymal Stem Cells. Human bone-marrow mesenchymal stem cells (hBM-MSCs) were isolated and cultured as previously described.[32,35] Briefly, bone marrow cells were obtained from washouts of the medullary cavities of the femurs of informed patients undergoing primary total hip replacement. Bone marrow was diluted with phosphate buffer saline (PBS) without Ca^{2+}/Mg^{2+} plus EDTA, mononuclear cells were isolated by density gradient on Lympholyte® (Cedarlane Laboratories Limited) and seeded in 25 cm^2 culture flasks at a density of 2.5×10^6 cells/mL in control medium, consisting of RPMI-1640 (Euroclone) medium containing 10% FBS, 2 m*M* of L-glutamine, and 100 U mL^{-1} of penicillin–streptomycin (Euroclone) in a humidified atmosphere and 5% carbon dioxide (CO_2) at 37°C. After 5 to 7 days, the non-adherent cells were removed, and fresh medium was added to the flasks. After 15 days, a fibroblast-like colony started to grow. The medium was changed every 3 days.

Cell Viability Assay. To evaluate the cell viability, hBM-MSCs were seeded on PLLA_SCPL, 1KM_SCPL, 1KA_SCPL, PLLA_TIPS_90:10, 1KM_TIPS_90:10 and 1KA_TIPS_90:10 substrates at a starting concentration of $2x10^3$ cells mL^{-1} in control medium, as previously described.[33,36] At different times (3, 7, 14 and 21 days), cell viability was measured by assaying the mitochondrial dehydrogenase activity through the XTT salt solution (Sigma) assay for 4 h at 37°C, according to the manufacturer's recommendations. The absorbance of the samples was measured using a microtiter plate reader (GDV) at 450 nm with a reference wavelength at 650 nm.

RESULTS AND DISCUSSION

Keratin Characterization

Figure 1(a,b) show the microstructures, observed by FESEM, of keratin powders extracted from Merino wool (a) and Brown Alpaca fibres (b) after the freeze-drying. Both KA and KM keratins showed a flake-like structure (due to the lyophilisation procedure[37]), as previously reported.[25,36] In order to study the keratin/1,4-dioxane interactions, keratin powder was dispersed in 1,4-dioxane and regenerated through solvent evaporation. The interaction of keratin with 1,4-dioxane was studied by analyzing the solvent effects on protein molecular weight distribution (protein degradation), and folding. For the sake of brevity, only the analysis carried out on keratin extracted from Merino wool will be reported. In Figure 1(c), the molecular weight distribution of keratin regenerated from 1,4-dioxane was compared with that of pristine keratin. As widely known, the electrophoretic pattern of pristine keratin [Figure 1(c), lane 1] shows two high-molecular-weight bands (60-45 kDa) of the low-sulfur intermediate filaments proteins (IFPs) and several low-molecular-weight bands (35-15 kDa) attributed to the high sulphur (HSPs) proteins of the matrix.[38] It can be observed that the electrophoretic pattern of the keratin regenerated from 1,4-dioxane [Figure 1(c), lane 2], suggests that the organic solvent does not induce any protein degradation.

The FT-IR spectroscopy was also used for the study of protein secondary structure. The keratin spectrum [Figure 2(a)] shows the characteristics adsorption bands of amides: the amide A (3300 cm^{-1}), related to the N—H stretching vibration, the amide I (1600–1700 cm^{-1}) due to the C=O stretching vibration, the amide II (1510–1580 cm^{-1}), due mainly to the in-plane NH bending and with the CN stretching vibration, and finally the amide III band (1200-1300 cm^{-1}) that is a complex vibrational band, dependent on the nature of side chains and hydrogen bonding environments.[39] The two intense peaks at 1195 and 1021 cm^{-1} are related to the asymmetric and symmetric stretching vibration of the Bunte salt residues formed during the keratin extraction procedure by sulphitolysis.[40] The Amide I band provides detailed information about the protein conformations, since its position and shape are determined by the protein backbone conformation.[41,42] In particular, the adsorption regions for the protein secondary structure represents the α-helix (1650–1658 cm^{-1}), the β-sheet (1621–1631 cm^{-1}) and the turns/random coil structures (1670–1697 cm^{-1}).[43] To study the

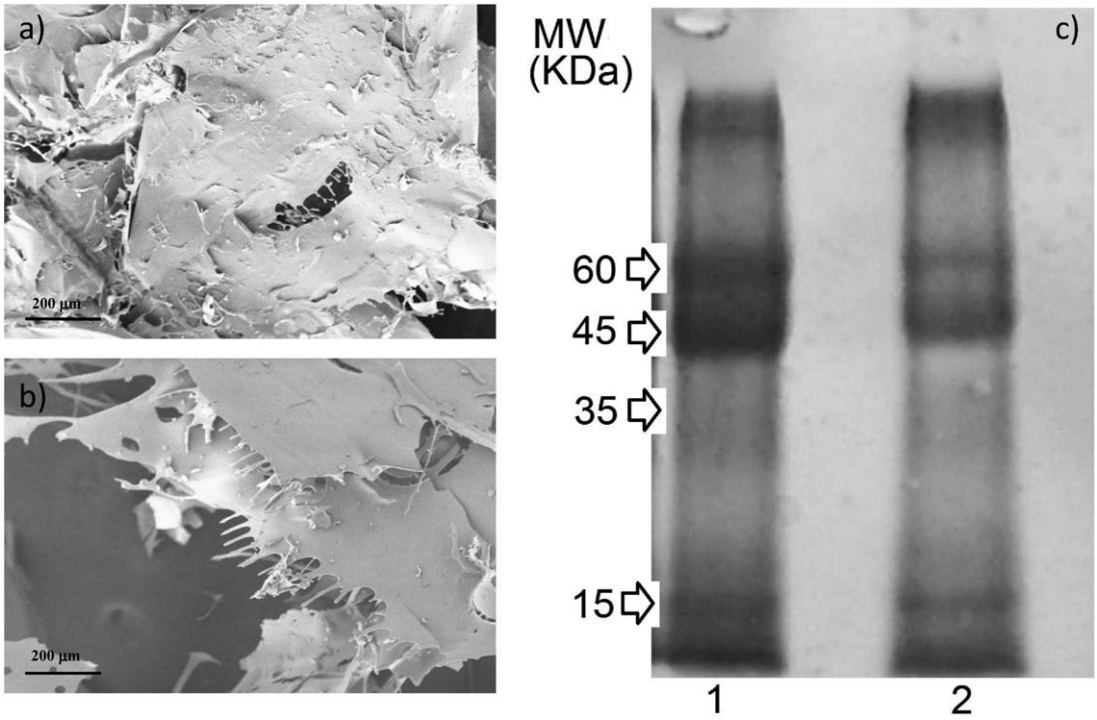

Figure 1. FESEM images of freeze-dried keratin powders extracted from (a) Merino wool and (b) Brown Alpaca fibres, (c) SDS-PAGE gel of untreated KM (lane 1) and KM treated with 1,4-dioxane (lane 2).

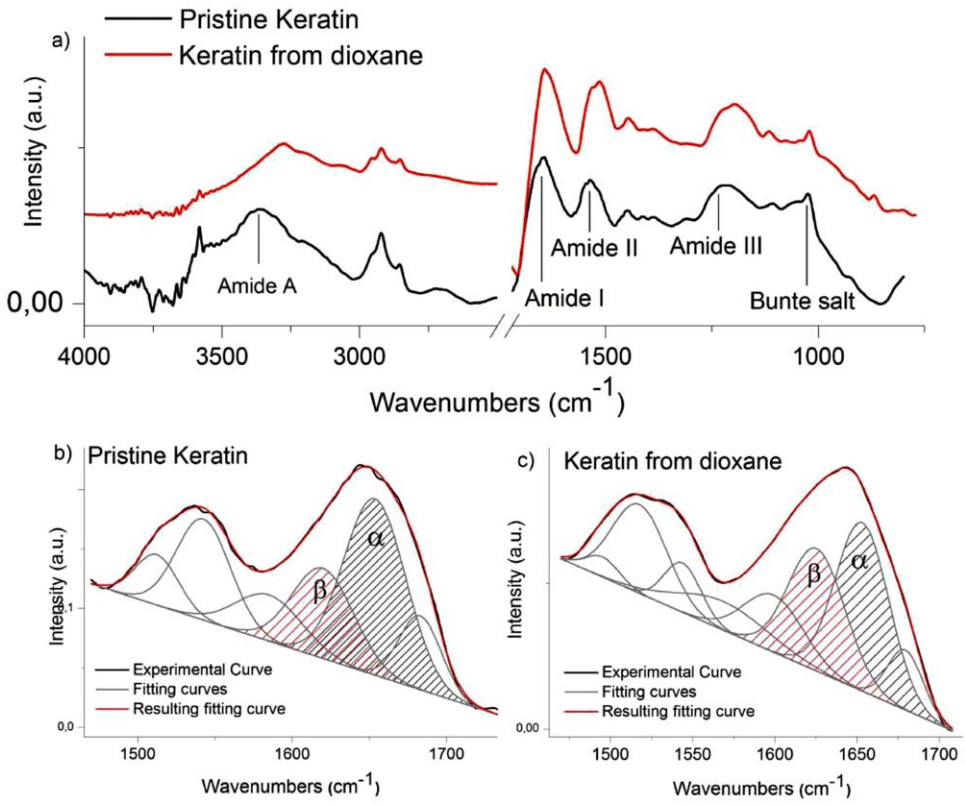

Figure 2. FTIR spectra of pristine KM and KM treated with 1,4-dioxane (a), peak resolution of Amide I region of pristine KM and KM regenerated in 1,4-dioxane (b,c). [Color figure can be viewed in the online issue, which is available at wileyonlinelibrary.com.]

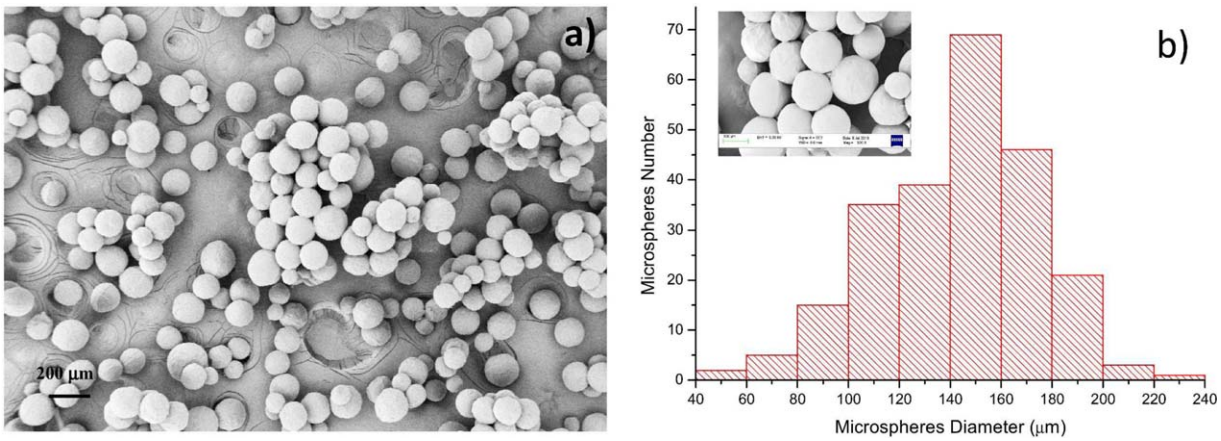

Figure 3. FESEM image of paraffin microspheres (a) and particle size distribution (b). [Color figure can be viewed in the online issue, which is available at wileyonlinelibrary.com.]

protein structural changes induced by the interaction of keratin with 1,4-dioxane, the amide I of the protein pristine keratin and keratin regenerated from the organic solvent were resolved into Gaussian bands [Figure 2(b,c)], whose number was defined in the second order derivative spectrum (data not shown). The contribution of each peak to the total band allows assigning the percentage of each secondary structure. As expected, in the case of pristine keratin, the percentage peak area related to the α-helix (48%) was higher than that of β-sheet structures (24%). As can be seen in Figure 2(c), the treatment of pristine keratin

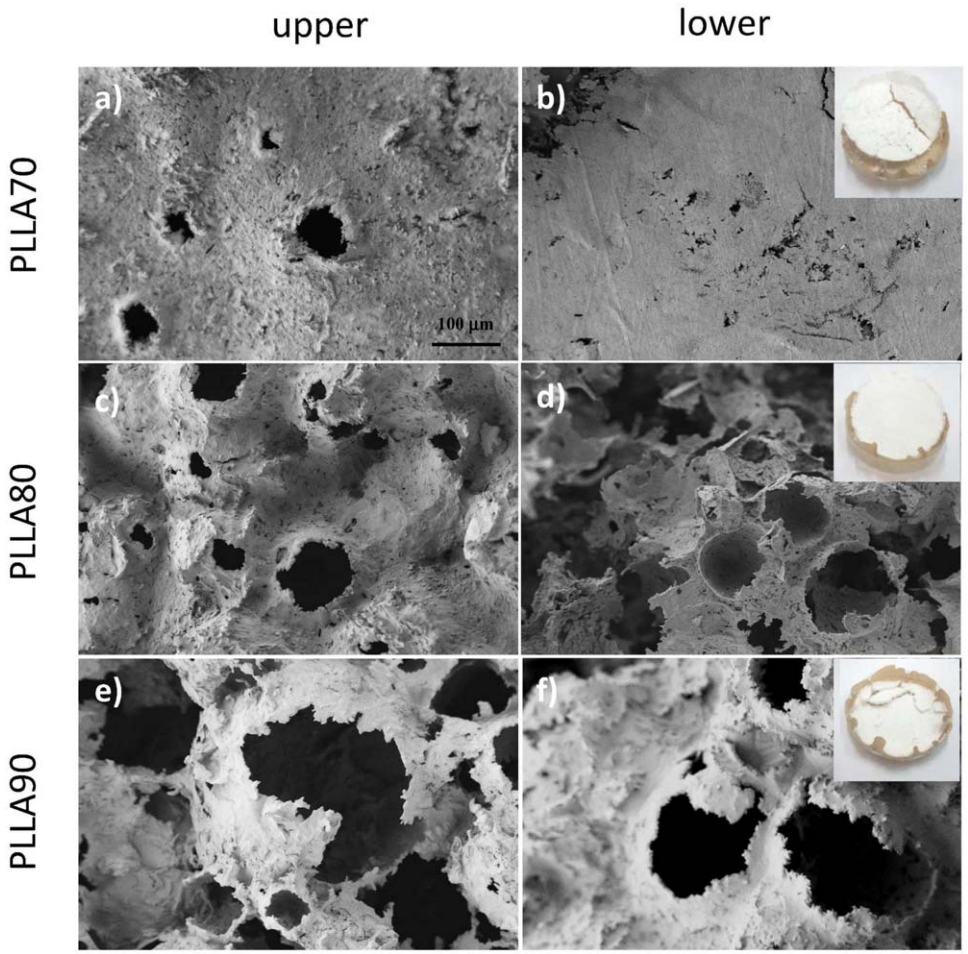

Figure 4. FESEM images of PLLA scaffolds surfaces produced by SCPL at different porosities: upper and lower surfaces for PLLA70 (a,b), PLLA80 (c,d) and PLLA90 (e,f). [Color figure can be viewed in the online issue, which is available at wileyonlinelibrary.com.]

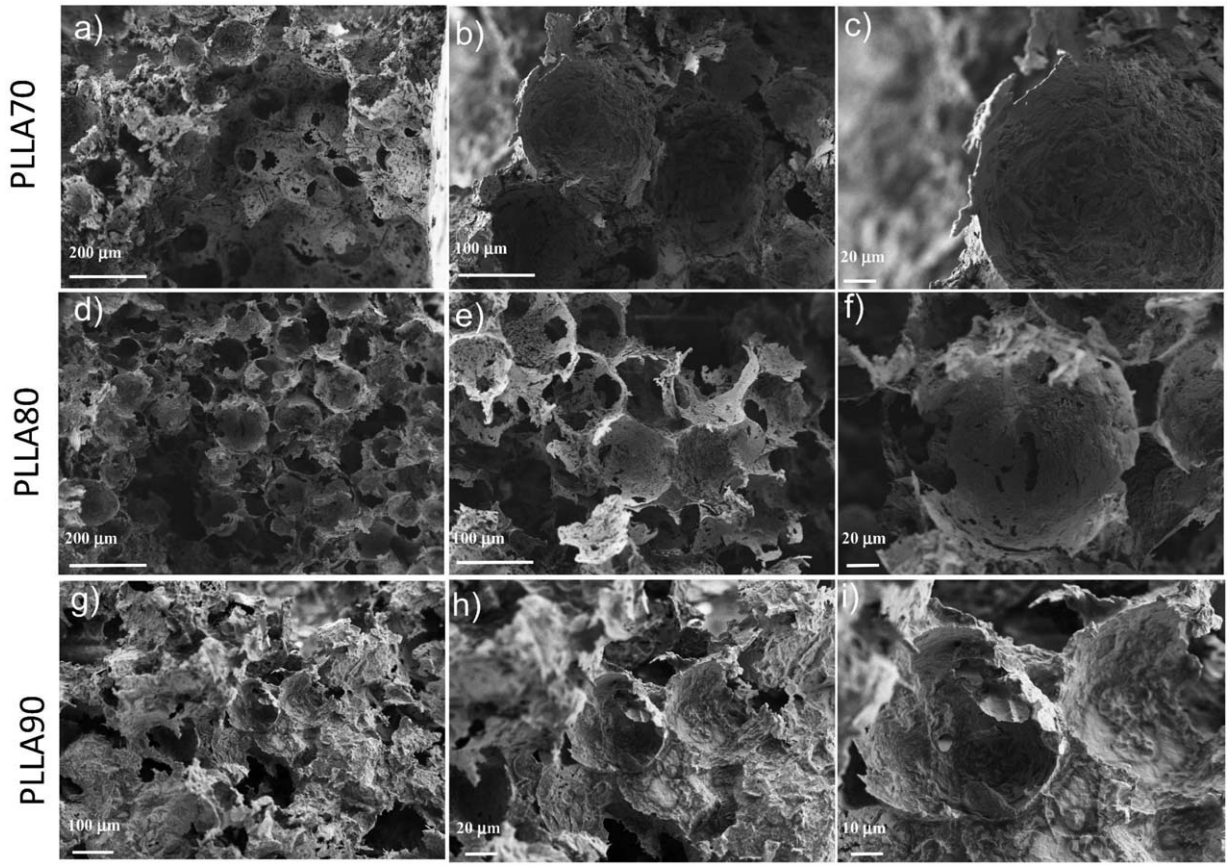

Figure 5. FESEM images of fractured surfaces of PLLA scaffolds produced by SCPL at different porosities: PLLA70 (a–c), PLLA80 (d–f) and PLLA90 (g–i).

with 1,4-dioxane causes an evident increase of the β-sheet structures (32%) and a corresponding decrease of the α-helices (42%). This behavior also observed for silk fibroin,[44] indicating that the organic solvent tends to favor a α -> β transition of the protein.

Porogen Characterization

The shape and size of synthesized paraffin microspheres used as porogen in SCPL process were analyzed by FESEM. The morphological investigation confirmed the uniform spherical distribution [Figure 3(a)], with smooth surface (insert) and size of the spheres controlled in the range of 80–200 μm [Figure 3(b)]. It has already been shown in the literature that the stirring rate and concentration of the PVA solution have a determinant effect in the control of size distribution and shape of the spheres. As reported by Ma *et al.*,[45] variable stirring rate and high PVA concentration resulted in smaller particles with uniform spherical shape, while a slower stirring rate and lower PVA concentration gave larger particles, including a certain portion of non-spherical particles.

Morphology of PLLA/Keratin Scaffolds Produced by SCPL

Effect of Porogen Content. The effect of different porogen content (70, 80 and 90 % wt) on surface and cross-section morphologies of produced PLLA scaffolds was investigated by FESEM. The images at different magnification are reported in Figure 4 (surfaces) and Figure 5 (cross sections). Both the lower (in contact with the *Teflon*® during the evaporation step) and the upper surface (exposed to the air) of PLLA70, PLLA80 and PLLA90 were investigated (Figure 4). The PLLA70 sample shows a less porous structure in both lower and upper surfaces [Figure 4(a,b)] with the presence of few pores, not completely homogenous, that characterized the upper surface. A different behavior was detected for PLLA80 [Figure 4(c,d)] and PLLA90 [Figure 4(e,f)] scaffolds, which appear highly porous, showing a well-interconnected structure. PLLA80 shows a continuous microstructure of well-interconnected pores, 50–100 μm in diameter and spherical shape that guarantees also the sample integrity [inset Figure 4(d)], not obtained in the case of PLLA90 [see inserts in Figure 4(f)], where pores with a higher and wider diameter distribution, were detected. The sample integrity was also compromised in the case of PLLA70 sample [inset Figure 4(b)].

The cross section images (Figure 5) of PLLA scaffolds confirm the same architecture through the scaffold thickness. For all different formulations, the pores reflected the negative of the paraffin microspheres. After dissolution and removal of the selected porogen, pores that corresponded in dimension to that of the used paraffin microspheres were observed [Figure 3(a,b)]. PLLA70 [Figure 5(a–c)] shows the presence of a discontinuous architecture with a non-homogeneous and wide distribution of pore shapes and sizes (100–150 μm in diameter). However, the pore walls, at higher magnification [Figure 5(c)],

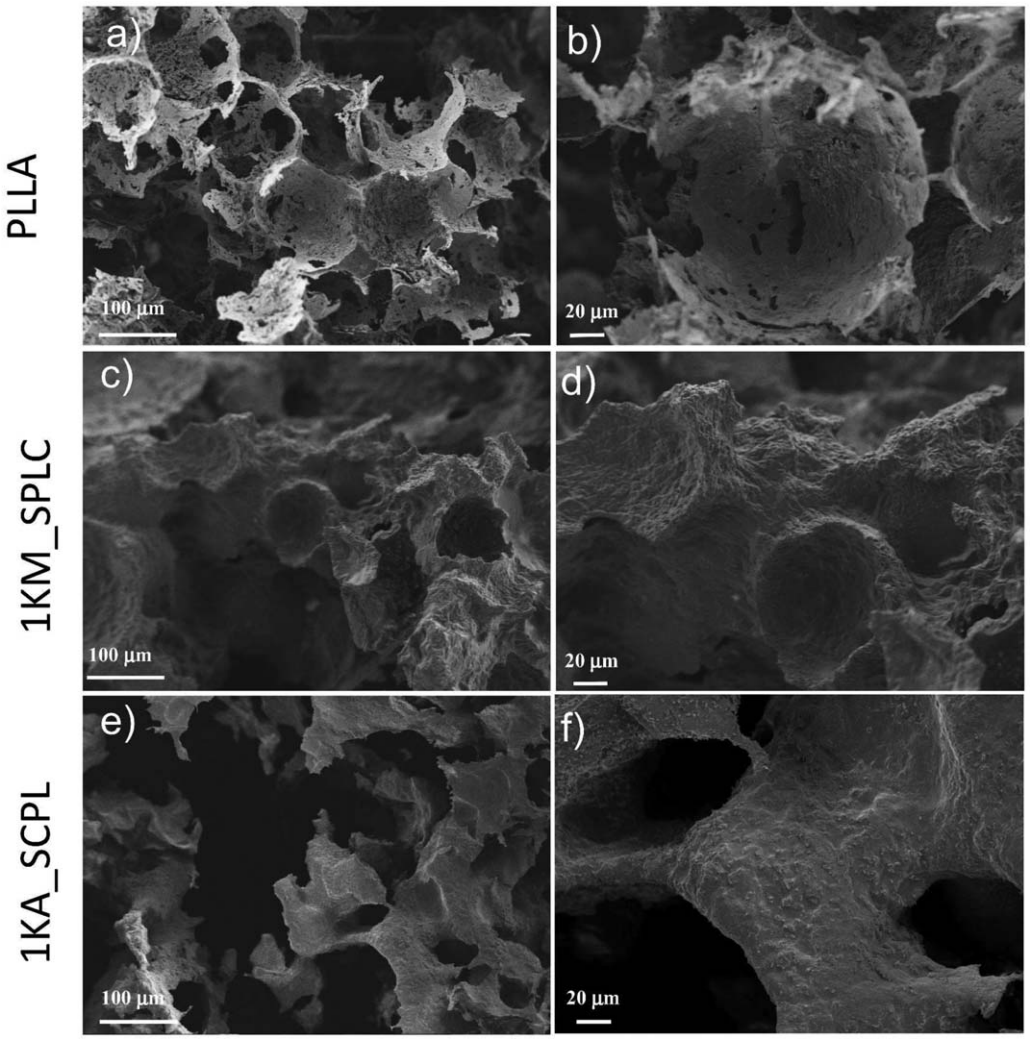

Figure 6. FESEM images of fractured surfaces of PLLA/keratin scaffolds produced by SCPL at 80% of porosity: neat PLLA (a,b), 1KM_SCPL (c,d) and 1KA_SCPL (e,f).

appear whole and with an evident micro-porosity. Furthermore, as previously detected for the surface characterization, an open porous architecture with rough pore sidewalls was detected for the PLLA90 scaffold formulation [Figure 5(f–h)]. On the contrary, PLLA80 shows a more uniform pore dimension distribution, the pore walls appear to be thicker and present the shape of the original paraffin microspheres [Figure 5(d–f)]. The hole diameter, centered at around 100–150 μm for the different formulations, could behave as channels for cells, nutrients, while the scaffold pore size could be tuned by choosing paraffin microspheres with different diameters (from 100 to 500 μm).[26] On the base of the discussed results, the PLLA80 scaffold was selected for the following production of PLLA/keratin-based three dimensional formulations.

Effect of Keratin Presence and Type. The effect of keratin presence and type on the cross section morphology of the PLLA80 scaffold (pore mean diameter estimated as 120 ± 30 μm, porosity $= 60 \pm 20\%$), was evaluated by FESEM (Figure 6) and the results for both 1KM_SCPL and 1KA_ SCPL are shown in Figure 6(c–f), respectively. Results showed that the pores had the circular shape of the original paraffin spheres with diameters within the pore size range for both 1KM_SCPL (pore mean diameter $= 120 \pm 30$ μm, porosity $45 \pm 15\%$) and 1KA_SCPL (pore mean diameter $= 150 \pm 30$ μm, porosity $= 35 \pm 15\%$) scaffolds. However, the addition of a small amount of KM (1 wt %) gave a scaffold morphology characterized by a more irregular structure with respect to the pure PLLA80 [Figure 6(a,b)], showing an open porous architecture in some points and a wider pore size distribution.[46] Moreover, between individual open cellular bigger pores, the presence of some smaller pores (diameters less than 100 μm) was also observed for 1KM_SCPL sample. Finally, 1KM_SCPL shows a rougher pore sidewall with respect to PLLA80 due to the presence of Merino wool keratin that modulates and influences the porous architecture formation [Figure 6(c,d)]. A similar behavior, with respect to the 1KM_SCPL, was also observed in the case of Alpaca keratin-based formulation. The presence of KA, in fact, does not influence the dimension of the pores, that mimics the porogen size, but a less interconnected porous architecture was

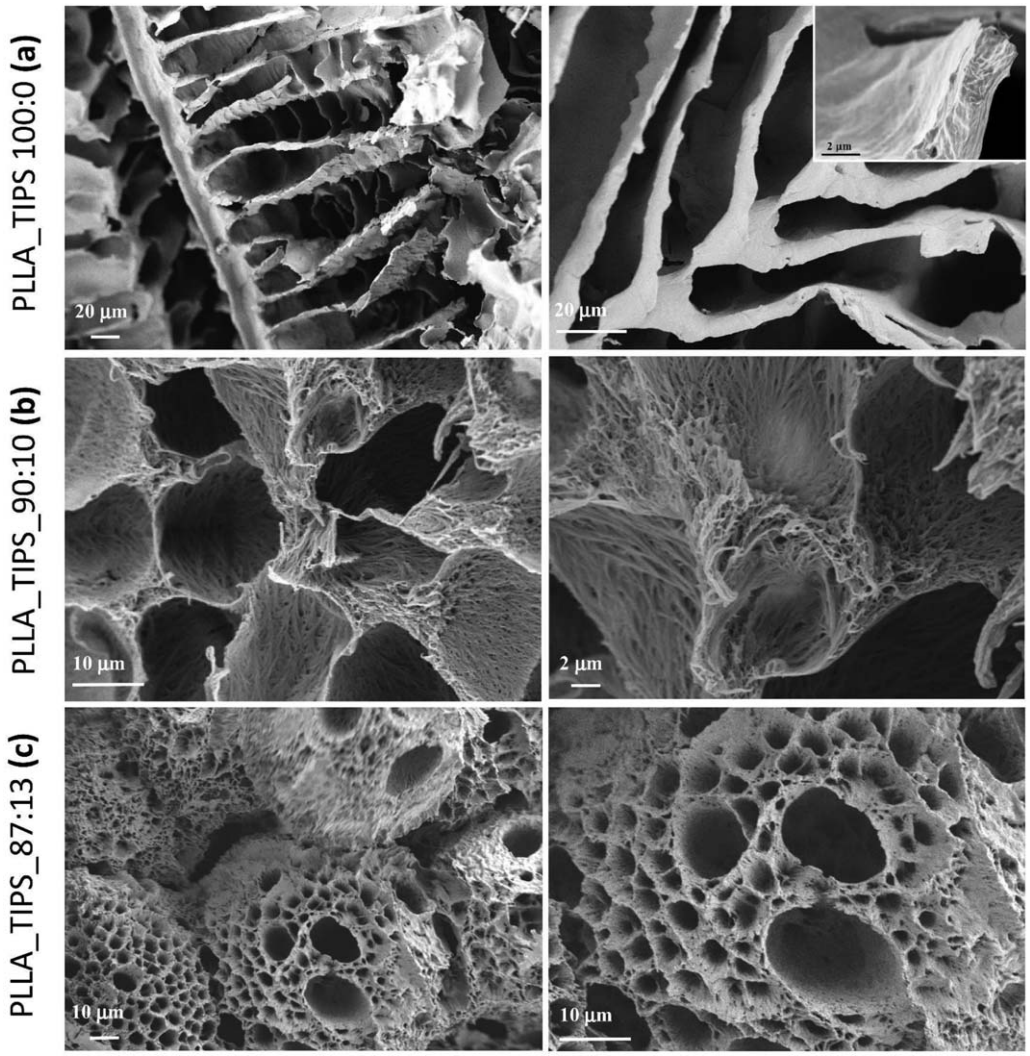

Figure 7. FESEM images of fractured surfaces of PLLA scaffolds produced by TIPS at different dioxane/water ratios: 100:0 (a), 90:10 (b) and 87:13 (c).

remarkably obtained in this specific case. This behavior could be ascribed to a less efficient dispersion of this type of keratin, as visible in Figure 6(f), in which the KA is clear detectable as white dots.

Morphology of Scaffolds Produced by TIPS

The TIPS scaffolds showed an open, porous and interconnected architecture with different pore sizes and morphologies, according to the selected process parameters. Furthermore, the filler presence and type (keratins from Merino Wool and Brown Alpaca) affect the morphology of the developed 3D polymeric biomaterials (see Figures 7–9).

The porous morphology of the scaffold is regulated by polymer and composite solution thermodynamic state. The porous morphology was obtained by a phase-separation mechanism, namely, solid–liquid (S–L) and liquid–liquid (L–L) phase separation.[23]

The morphology is function of various processing parameters, including quenching temperature, polymer concentration, solvent composition, and aging time. In our process, we fixed some parameters, as described in the material and methods section, since the main aim of this work was to study how keratin type and solvent ratio could affect the PLLA scaffold morphology.

Effect of Solvent Dilution. The composition of the 1,4-dioxane/water solution is one of the main parameters affecting the PLLA and composite scaffold microstructure. The morphology and microstructure of the scaffolds developed by TIPS procedure were examined using FESEM, as shown in (Figures 7–9).

Figure 7 shows the FESEM images at different resolution of PLLA scaffolds developed by using different 1,4-dioxane/water mixtures: PLLA_TIPS_100:0 (a), PLLA_TIPS_90:10 (b), PLLA_TIPS_87:13 (c). When 1,4-dioxane was used alone, the porous structure was obtained by solid–liquid phase separation of the polymer solution. During the quenching step, the solvent was able to crystallize and the polymer was removed from the solvent crystallization front. Consequently, crystallized and sublimated solvent evolved to pores, which characteristics are determined by crystals morphologies during the quenching event. The temperature gradient along the solvent crystallization

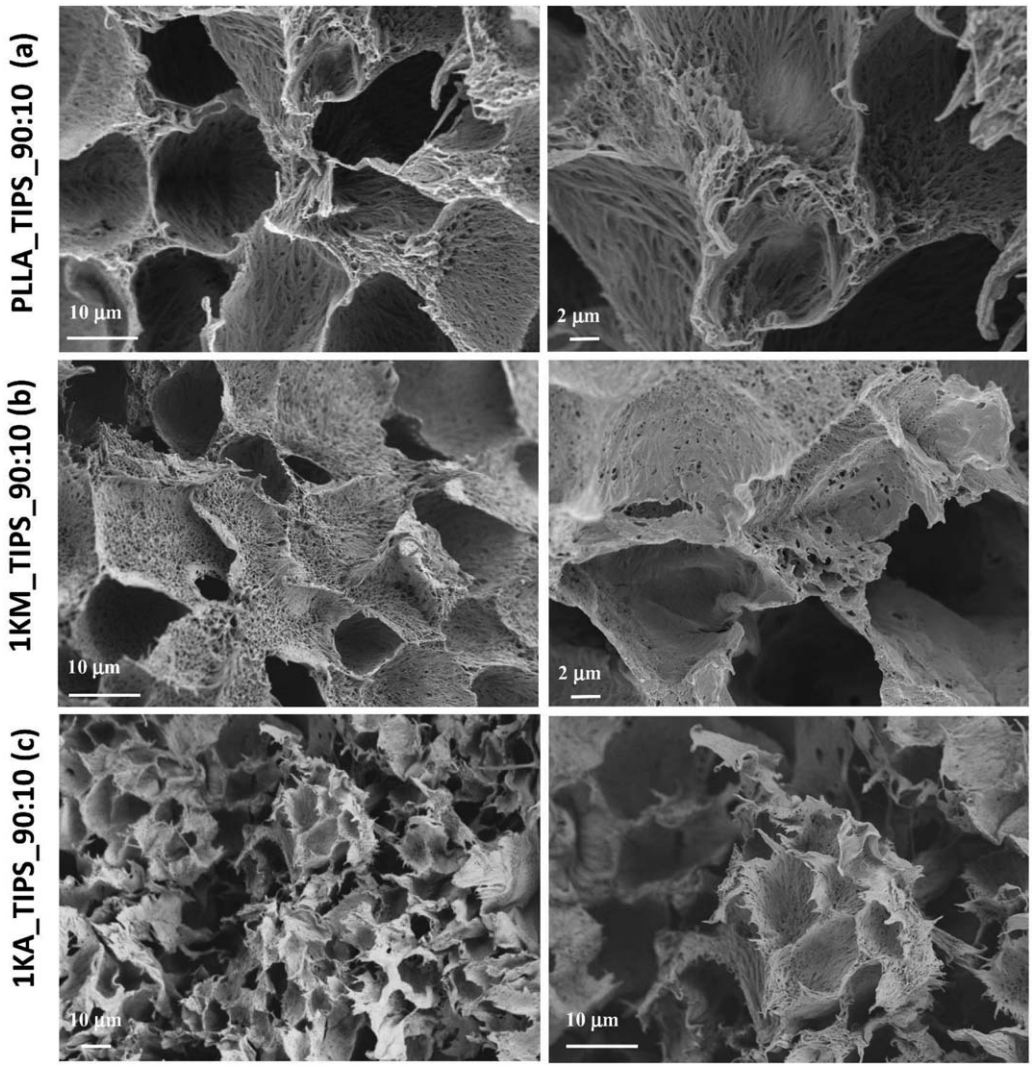

Figure 8. FESEM images of fractured surfaces of PLLA/keratin scaffolds produced by TIPS at 90:10 (1,4-dioxane/water): neat PLLA (a), 1KM_TIPS_90:10 (b) and 1KA_TIPS_90:10 (c).

direction led to an anisotropic structure. The PLLA scaffold fabricated with pure 1,4-dioxane showed a ladder-like pore structure, a morphology typically observed in PLLA formed by solid–liquid phase separation.[20,23,47] The foam [Figure 7(a)] shows a morphology with parallel tubes; the internal wall of these channels is also macroporous, and shows a general pattern of lamellae radially oriented from a central hole. Some of the interlamellar regions are also subdivided into pores, the diameter of which is about 10 μm. A higher magnification image reveals the significant regularity and directionality of the pores with the specific substructure of the lamellae, with dense pore walls.

Quite different morphologies appeared in the PLLA scaffolds fabricated with 1,4-dioxane and water/solvent mixture systems [Figure 7(b,c)]. The proportion of water in the solvent systems had a significant effect on the pore size and overall morphology of the scaffolds. For the systems with a mixture of 1,4-dioxane/water, spherical pore morphology is observed (pore diameter ranging from 10 to 30 μm) [Figure 7(b,c)], replacing the regular ladder-like pore structure, with the pore size and morphology affected by the composition of the solvent mixture (PLLA_TIPS_90:10 and PLLA_TIPS_87:13). Another observed change was the pore wall surface texture. While relatively smooth pore morphology of PLLA scaffolds prepared from a mono-solvent system can be observed, in the case of scaffolds prepared from a mixed solvent system a fibrous network is visible. In addition, when using the 1,4-dioxane/water mixture solvent, the scaffolds consisted of three ranges of pore sizes: spherical micropores from 10 to 30 μm, smaller pore of around 1 lm between the bigger pores, and a nanoporous structure evident on the wall of the pores, due to the fibrous network structure obtained. For the system with lower water content in the solvent mixture [PLLA_TIPS_90/10, Figure 7(b)], the scaffold pore size decreases, if compared with the parallel system [PLLA_TIPS_87/13, Figure 7(c)]. A decrease in water content in the solution results in higher solubility that increases the solution viscosity. The high viscosity and decreased driving force decelerate the rate of phase separation in the TIPS process.[48]

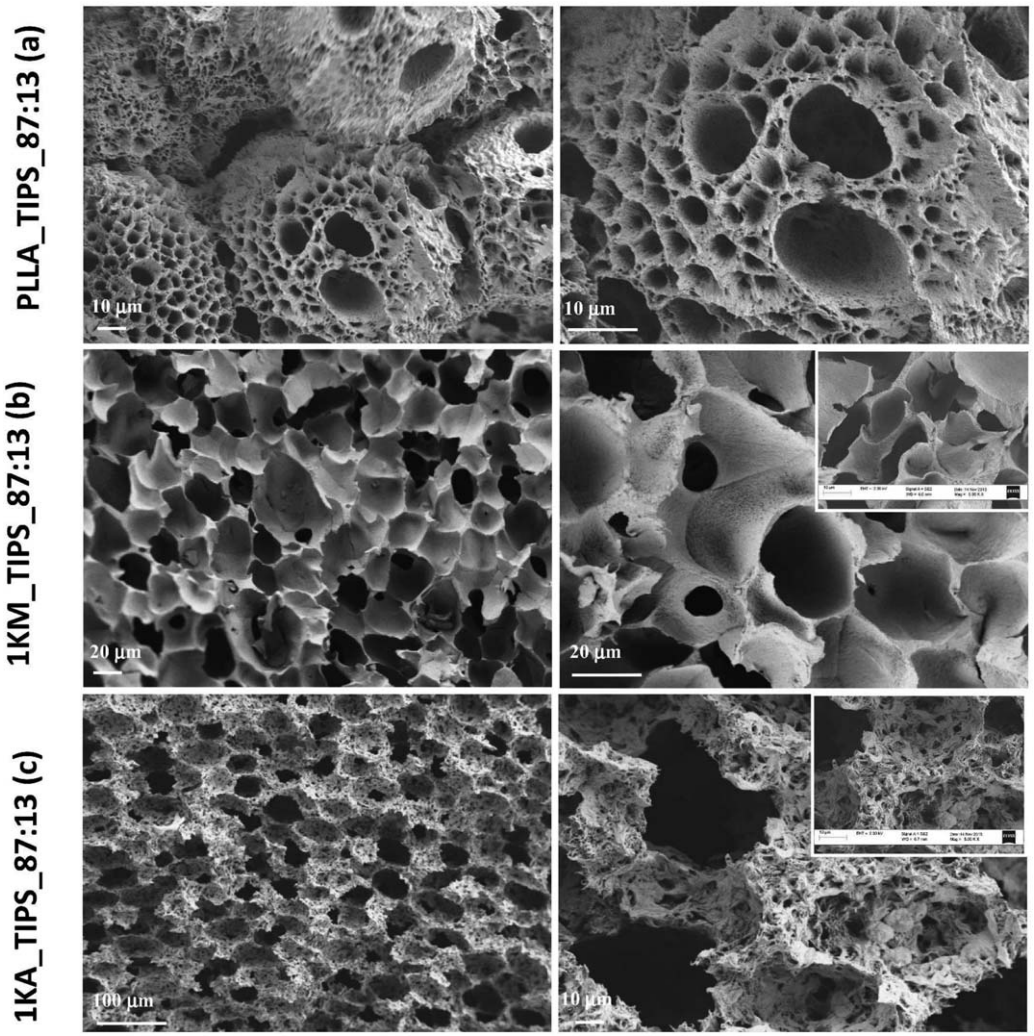

Figure 9. FESEM images of fractured surfaces of PLLA/keratin scaffolds produced by TIPS at 87:13 (1,4-dioxane/water): neat PLLA (a), 1KM_TIPS_87:13 (b) and 1KA_TIPS_87:13 (c).

Effect of the Keratin Type. Figure 8 shows the morphology of the composite scaffold cross sections, produced using 1 wt % of KM and KA, with 90:10 1,4-dioxane/water solution mixture, compared with pure PLLA (PLLA_TIPS_90:10) fabricated in the same conditions.

The introduction of keratin fibers from Merino wool and Brown Alpaca into the polymer solution perturbed the solvent crystallization. As predicted, the composite scaffold exhibited an isotropic and irregular pore structure. The perturbation by keratin fibers at this low weight content (1 wt %) was small. As a result, 1KM_TIPS_90:10 (pore mean diameter (14 ± 3) μm, porosity = 20 ± 8%) and 1KA_TIPS_90:10 (pore mean diameter (9 ± 1) μm, porosity = 10 ± 3%) composite scaffolds maintained the main characteristic of the PLLA developed with the same 1,4-dioxane/water ratio (90:10) (pore mean diameter (19 ± 1) μm, porosity = 45 ± 15%).

A more homogeneous microstructure was observed in the case of the biocomposite developed with KM (1KM_TIPS_90:10), that shows spherical pore morphology with a diameter of 20–30 μm, and interstitial nanopores between the main micropore structure. Furthermore, the presence of fibrous polymer configuration is evident by analyzing the pore walls.[44] The surface/volume ratio of fibrous scaffolds is greater than the one in scaffolds with solid pore walls, which might increase the protein adsorption capacity.

Figure 9 shows the composite scaffold morphology produced using 1 wt % of KM and KA, with 87:13 of 1,4-dioxane/water mixture (1KM_TIPS_87:13 and 1KA_TIPS_87:13, respectively), compared with neat PLLA (PLLA_TIP_87:13) developed in the same conditions. A more evident fibrous-like morphology was observed in the KA scaffold fabricated with the 87:13 of 1,4-dioxane/water mixture. The pores show good interconnectivity, increased pore size (around 50 μm), and an open structure between pore and on the pore wall. The difference between the two used keratins could be ascribed to the different thermal behavior of the keratins observed in PLLA dense biocomposite systems.[25] Keratin from Alpaca fibres can act as nucleating agents in the formation of PLLA crystals in the heating phase,

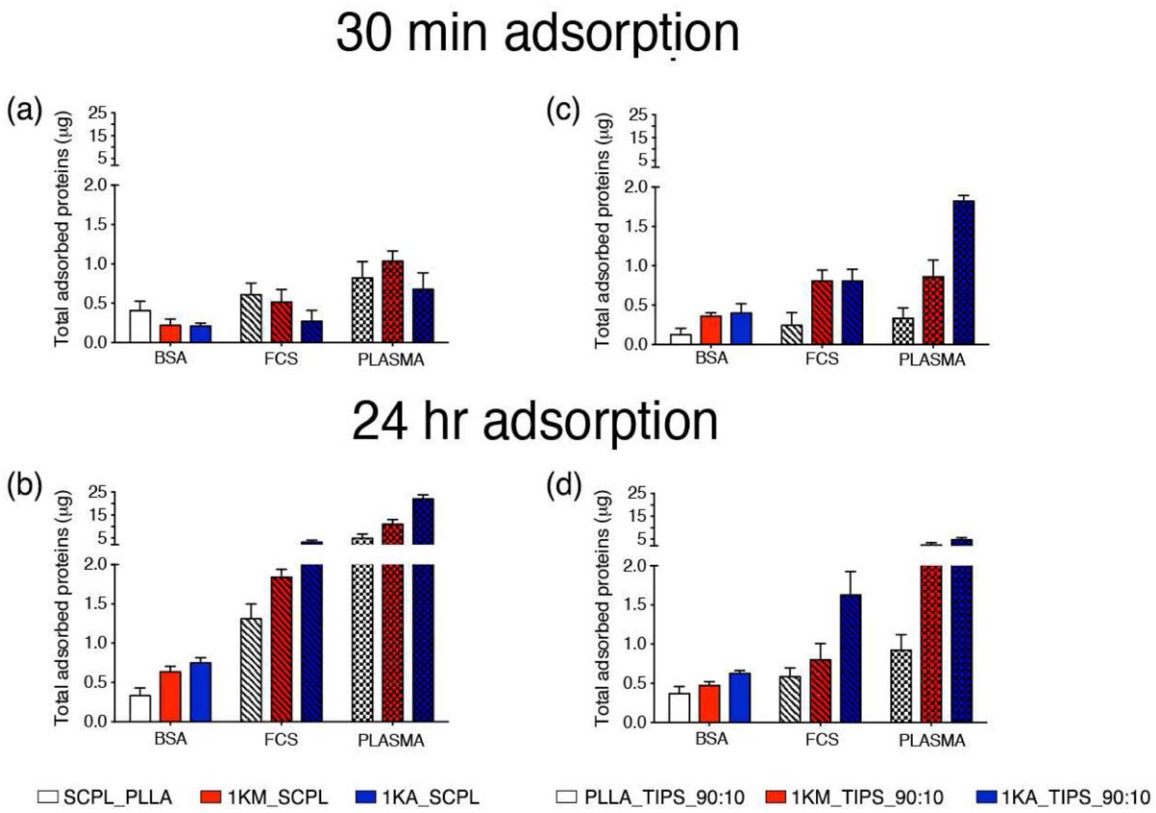

Figure 10. Protein adsorption on PLLA_SCPL, 1KM_SCPL, 1KA_SCPL, PLLA_TIPS_90:10, 1KM_TIPS_90:10, and 1KA_TIPS_90:10 biocomposite scaffolds after 30 min (a,c) and 24 h (b,d). [Color figure can be viewed in the online issue, which is available at wileyonlinelibrary.com.]

with a higher crystallization degree, as observed in our previous work.[25] The increased porosity could make 1KA_TIPS scaffold suitable for cell culture penetration inside the pores, while the nanopore structure observed in the pore wall could be suitable for nutrient flow.

Biological Characterization

Figure 10 shows the protein adsorption on PLLA_SCPL, 1KM_SCPL, 1KA_SCPL, PLLA_TIPS_90:10, 1KM_TIPS_90:10, 1KA_TIPS_90:10 films after 30 min and 24 h of protein incubation. Compared to PLLA, we measured a comparable concentration of BSA, FBS 10% and plasma (dilution 1:10) on 1KM_SCPL and 1KA_SCPL after 30 min of adsorption [Figure 10(a)], whereas we detected an increase of protein adsorption on SCPL PLLA/K-derived composite films compared to neat PLLA after 24h either of BSA, or FBS 10% and plasma (dilution 1:10) protein incubation. Here, we found the most significant increase on the adsorption of FCS 10% on 1KA_SCPL composite film [Figure 10(b)].

Interestingly, the trend of adsorption of BSA, FBS 10% and plasma (dilution 1:10) on PLLA_TIPS_90:10, 1KM_TIPS_90:10 and 1KA_TIPS_90:10 was similar after 30 min of and 24h protein incubation, however with some differences between samples [Figure 10(c,d)]. We detected a comparable level of BSA adsorption on PLLA_TIPS_90:10, 1KM_TIPS_90:10 and 1KA_TIPS_90:10 [Figure 10(c,d)], whereas we found an increase of FBS 10% and plasma adsorption on 1KM_TIPS_90:10 and 1KA_TIPS_90:10 compared to PLLA_TIPS_90:10 [Figure 10(c,d)]. The highest level of FBS 10% was found in 1KA_TIPS_90:10 at 24 h. More significant was the increase of plasma (dilution 1:10) adsorption in 1KM_TIPS_90:10 and 1KA_TIPS_90:10 with respect to PLLA_TIPS_90:10. In this case, we observed a trend in the order 1KA_TIPS_90:10 > 1KM_TIPS_90:10 > PLLA_TIPS_90:10 after 30 min of plasma incubation [Figure 10(c)], whereas we noted a trend in the order 1KA_TIPS_90:10 = 1KM_TIPS_90:10 > PLLA_TIPS_90:10 after 24 h of plasma [Figure 10(d)].

These data suggest that the characteristics of 90/10 PLLA/K-derived samples could influence the protein adsorption, perhaps as consequence of the different morphology and scaffold macro and microstructure induced by the process technology and the presence of different kinds of keratin.

Stem Cell Viability on PLLA and PLLA/Keratin Biocomposites. To evaluate the biocompatibility of the materials, hBM-MSCs were seeded on PLLA, 1KA_SCPL, 1KM_SCPL, PLLA_TIPS_90:10, 1KM_TIPS_90:10 and 1KA_TIPS_90:10 composites at a starting concentration of 2×10^3 cells mL^{-1} in control medium. We observed a decrease in the level of mitochondrial dehydrogenase activity in stem cells cultured ether in SCPL PLLA, SCPL PLLA/keratin-based biofilms or in PLLA_90:10 and 90:10_PLLA/keratin-based samples compared to tissue culture plastic (TCP), selected as control [Figure 11(a,b)]. No sign of toxicity was detected in all stem cell-biofilm cultures (data not shown), indicating that the characteristics of the materials are safe for stem cells, and in turn that PLLA_SCPL, SCPL_PLLA/keratin-based biofilms and

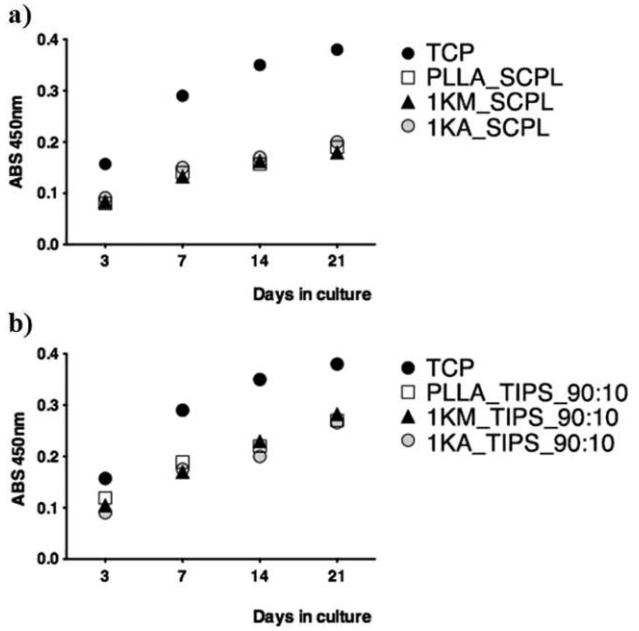

Figure 11. XTT viability assay of hBM-MSCs on TCP, PLLA_SCPL, 1KM_SCPL, 1KA_SCPL (a) and PLLA_TIPS_90:10, 1KM_TIPS_90:10, and 1KA_TIPS_90:10 (b) at 3, 7, 14 and 21 days.

PLLA_TIPS_90:10, 90:10_TIPS_PLLA/keratin-based biofilms are suitable substrates for human adult stem cell cultures.

CONCLUSIONS

PLLA porous scaffolds were successfully developed using two solvent assisted processes: the SCPL process (using paraffin spheres as porogen) and the TIPS process. It has been shown that various microcellular and porous foam morphologies can be obtained using both SCPL and TIPS by adjusting the process parameters. A slight change in the parameters, such as porogen content or solvent/no solvent ratio, significantly affected the resultant foam morphology. Keratins extracted from two different sources (Merino wool and Brown Alpaca) were regenerated in 1,4-dioxane, proving that the selected organic solvent does not induce any protein degradation. The addition of keratin fibres could provide a new method for preparing macroporous biocomposite scaffolds. This characteristic architecture is crucial for biological applications, because it allows a favorable distribution of biological molecules (TIPS based scaffolds), as well as cell ingrowth (SCPL based scaffolds), one of the necessary steps for tridimensional organization of stem cells for the generation of artificial tissue. We suggest that the foams prepared by SCPL could be suitable for cell ingrowth, while scaffolds produced using TIPS could find applications in controlled drug delivery. Here we have demonstrated the biocompatibility of both composites, that seem to be suitable substrates for adult bone-marrow mesenchymal stem cell cultures.

ACKNOWLEDGMENTS

The authors acknowledge Gianni Berna of Società Agricola Maridiana, for the Brown Alpaca fibres supply, and Lanificio Cariaggi—fine yarns, for the Merino wool fibres supply.

REFERENCES

1. Kirfel, J.; Magin, T. M.; Reichelt, J. *Cell. Mol. Life Sci.* **2003**, *60*, 56.
2. Aluigi, A.; Tonetti, C.; Tonin, C.; Casasola, R.; Ferrero, F. *J. Biobased Mater.* **2012**, *6*, 230.
3. Altman, G. H.; Diaz, F.; Jakuba, C.; Calabro, T.; Horan, R. L.; Chen, J.; Lu, H.; Richmond, J.; Kaplan, D. L. *Biomaterials* **2003**, *24*, 401.
4. Goo, H. C.; Hwang, Y. S.; Choi, Y. R.; Cho, H. N.; Suh, H. *Biomaterials* **2003**, *24*, 5099.
5. Yamauchi, K.; Maniwa, M.; Mori, T. *J. Biomater. Sci. Polym. Ed.* **1998**, *9*, 259.
6. Balaji, S.; Kumar, R.; Sripriya, R.; Kakkar, P.; Vijaya Ramesh, D.; Neela Kanta Reddy, P.; Sehgal, P. K. *Mater. Sci. Eng., C* **2012**, *32*, 975.
7. Peter, S. J.; Miller, M. J.; Yasko, A. W.; Yaszemski, M. J.; Mikos, A. G. *J. Biomed. Mater. Res.* **1998**, 422.
8. Suh, H.; Hwang, Y. S.; Lee, J. E.; Han, C. D.; Park, J. C. *Biomaterials* **2001**, *22*, 219.
9. Quirk, A. R.; Chan, W. C.; Davis, M. C.; Tendler, S. J. B.; Shakesheff, K. M. *Biomaterials* **2001**, *22*, 865.
10. Kim, B. S.; Park, K. E.; Park, W. H.; Lee, J. *Biomed. Mater.* **2013**, *8*, 045006.
11. Xu, H.; Cai, S.; Xu, L.; Yang, Y. *Langmuir* **2014**, *30*, 8461.
12. Yuan, J.; Shen, J.; Kang, I.-K. *Polym. Int.* **2008**, *57*, 1188.
13. Li, J. S.; Li, Y.; Li, L.; Mak, A. F. T.; Ko, F.; Qin, L. *Adv. Mater. Res.* **2008**, 845.
14. Dhandayuthapani, B.; Yoshida, Y.; Maekawa, T.; Sakthi Kumar, D. *Int. J. Polym. Sci.* **2011**, doi: 10.1155/2011/290602.
15. Selvam, S.; Chang, W. V.; Nakamura, T.; Samant, D. M.; Thomas, P. B.; Trousdale, M. D.; Mircheff, A. K.; Schechter, J. E.; Yiu, S. C. *Tissue Eng. Part C Methods* **2009**, *15*, 463.
16. Budyanto, L.; Goh, Y. Q.; Ooi, C. P. *J. Mater. Sci. Mater. Med.* **2009**, *20*, 105.
17. Armentano, I.; Ciapetti, G.; Pennacchi, M.; Dottori, M. S.; Devescovi, V.; Granchi, D.; Baldini, N.; Olalde, B.; Jurado, M. J.; Marquinez Alava, J. I.; Kenny, J. M. *J. Appl. Polym. Sci.* **2009**, *114*, 3602.
18. Rezwan, K.; Chen, Q. Z.; Blaker, J. J.; Boccaccini, A. R. *Biomaterials* **2006**, *27*, 3413.
19. Boccaccini, A. R.; Maquet, V. *Compos. Sci. Technol.* **2003**, *63*, 2417.
20. Ma, P. X.; Zhang, R. *J. Biomed. Mater. Res.* **2001**, *56*, 469.
21. Maquet, V.; Martin, D.; Scholtes, F.; Franzen, R.; Schoenen, J.; Moonen, G.; Jerome, R. *Biomaterials* **2001**, *22*, 1137.
22. Kim, H. D.; Bae, E. H.; Kwon, I. C.; Ramsurat Pal, R.; Nam, J. D.; Lee, D. S. *Biomaterials* **2004**, *25*, 2319.
23. He, L.; Zuo, Q.; Shi, Y.; Xue, W. *J. Appl. Polym. Sci.* **2013**, 131.
24. Martinez-Perez, C. A.; Olivas-Armendariz, I.; Castro-Carmona, J. S.; Garcia-Casillas, P. E. in Advances in Regenerative Medicine, Dr Sabine Wislet-Gendebien, Ed.,

2011, ISBN: 978-953-307-732-1, Scaffolds for Tissue Engineering Via Thermally Induced Phase Separation.

25. Aluigi, A.; Tonetti, C.; Rombaldoni, F.; Puglia, D.; Fortunati, E.; Armentano, I.; Santulli, C.; Torre, L.; Kenny, J. M. *J. Mater. Sci.* **2014**, *49*, 6257.
26. Li, J.; Li, Y.; Li, L.; Mak, A. F. T.; Ko, F.; Qin, L. *Compos. Part B* **2009**, *40*, 664.
27. Li, J. S.; Beaussart, A.; Chen, Y.; Mak, A. F. T. *J. Biomed. Mater. Res.* **2007**, *80*, 226.
28. Li, J. S.; Mak, A. F. T. *Compos. Part B* **2007**, *38*, 317.
29. Laemmli, U. K. *Nature* **1970**, *227*, 680.
30. Marshall, R. C. *Text. Res. J.* **1981**, *51*, 106.
31. Choudhury, M.; Mohanty, S.; Nayak, S. *J. Tissue Sci. Eng.* **2014**, *6*, 142.
32. D'Angelo, F.; Armentano, I.; Mattioli, S.; Crispoltoni, L.; Tiribuzi, R.; Cerulli, G. G.; Palmerini, C. A.; Kenny, J. M.; Martino, S.; Orlacchio, A. *Eur. Cell Mater.* **2010**, *20*, 231.
33. Montesano, S.; Lizundia, E.; D'Angelo, F.; Fortunati, E.; Mattioli, S.; Morena, F.; Bicchi, I.; Naro, F.; Sampaolesi, M.; Sarasua, J. R.; Kenny, J. M.; Orlacchio, A; Armentano, I.; Martino, S. *Tissue Eng.* **2013**, Article ID 825912.
34. Bradford, M. M. *Anal. Biochem.* **1976**, *72*, 248.
35. Martino, S.; D'Angelo, F.; Armentano, I.; Tiribuzi, R.; Pennacchi, M.; Dottori, M. S.; Mattioli, S.; Caraffa, A.; Cerulli, G. G.; Kenny, J. M.; Orlacchio, A. *Tissue Eng. A* **2009**, *15*, 3139.
36. Fortunati, E.; Aluigi, A.; Armentano, I.; Morena, F.; Emiliani, C.; Martino, S.; Santulli, C.; Torre, L.; Kenny, J. M.; Puglia, D. *Mater. Sci. Eng., C* **2015**, *47*, 394.
37. Cardamone, J. M.; Nunez, A.; Garcia, R. A.; Aldema-Ramos, M. *Lett. Mater. Sci.* **2009**.
38. Maclaren, J. A.; Milligan, B. Wool Science, 1; Science Press: **1981**, 1.
39. Wojciechowska, E.; Włochowicz, A.; Wesełucha-Birczynska, A. *J. Mol. Struct.* **1999**, *307*, 511.
40. Erra, P.; Gómez, N.; Dolcet, L. M.; Juliá, M. R.; Lewis, D. M.; Willoughby, J. H. *Textile Res. J.* **1997**, *67*, 397.
41. Aluigi, A.; Zoccola, M.; Vineis, C.; Tonin, C.; Ferrero, F.; Canetti, M. *Int. J. Biol. Macromol.* **2007**, *41*, 266.
42. Feughelman, M.; Lyman, D. J.; Willis, B. K. *Int. J. Biol. Macromol.* **2002**, *30*, 95.
43. Stuart, B. Biological Applications of Infrared Spectroscopy; John Wiley & Sons: Chichester, West Sussex, England, **1997**.
44. Izuka, E. *Protein Struct.* **1968**, *160*, 454.
45. Ma, P. X.; Choi, J. W. *Tissue Eng.* **2001**, *7*, 23.
46. Armentano, I.; Dottori, M.; Fortunati, E.; Villarreal, E.; Chávez, J. L.; Arzate, H.; Kenny, J. M. *J. Nanostruct. Polym. Nanocompos.* **2012**, *8*, 12.
47. Zhang, R.; Ma, P. X. *J. Biomed. Mater. Res.* **1999**, *44*, 446.
48. Hua, F. J.; Kim, G. E.; Lee, J. D.; Son, Y. K.; Lee, D. S. *J. Biomed. Mater. Res.* **2002**, *63*, 161.
49. Ma, P. X.; Zhang, R. *J. Biomed. Mater. Res.* **1999**, *46*, 60.